Characterization of Particle Rebound Phenomena in the Erosion of Turbomachinery

Jonathan A. Laitone*
University of Michigan, Ann Arbor, Michigan

The rebound of solid particles on material surfaces typical to jet turbines is predicted to assess the frequency of multiple impacts and secondary erosion. The numerical solution models boundary-layer growth, separation, and unsteady wake effects in the gas flow. The microgeometry of the surface is taken into account via experimentally determined statistical boundary conditions applied to the particle phase. The three types of rebound phenomena identified include imbedment, single-impact rebound, and multiple impacts, which appear similar to the way a stone skips across water. The momentum change after impact is characterized with respect to primary and secondary erosion mechanisms. The secondary erosion is found to increase with particle size. This result is in part an aerodynamic effect.

Nomenclature

$\mathcal{R}$ = aspect ratio = σ/R
C_D = drag coefficient of particle
d = particle diameter
k = time step (dimensionless)
R = cylinder radius
Re = flow Reynolds number = $U2R/\nu$
Re_p = particle Reynolds number = $|u-u_p|d/\nu$
q = particle impact speed
t = time (dimensionless)
U = gas free stream speed
u = gas velocity vector (dimensionless)
u_p = particle velocity vector (dimensionless)
α = particle impact angle (measured from the surface)
α_0 = particle volume fraction
β = particle rebound angle (measured from the surface)
δ^* = average displacement thickness of boundary layer
δ_l = relative density of particles to gas
θ = cylinder angle (measured from the front stagnation point)
λ = inertia number
μ = gas viscosity
ν = gas kinematic viscosity
ρ = gas density
ρ_p = particle material density
σ = particle radius

Subscripts

N = normal direction
p = particle phase
T = tangential direction

Introduction

THE erosive wear of material surfaces exposed to liquid droplets and solid particles has received wide attention owing to the financial loss associated with this wear mechanism. Over 40 years ago, Taylor[1] investigated raindrops impinging on aircraft wings in an effort to reduce icing. The equations he developed for the droplet flow still apply to many problems in modern turbomachinery. Turbines used in jet aircraft, hovercraft, and helicopters operating in dusty or sandy environments may have service lives reduced to 100 h by the erosion of turbine blades.[2]

Current interest in energy conversion systems has focused attention on gas-particle flows. Reducing erosion in fluidized beds and advanced coal-fired combustors is crucial for their successful development.

Although many experimental studies have been conducted, there is a lack of erosion models due to the inherent complexity of each specific case. In the past this has necessitated isolating particular problem areas such as the particle boundary-layer interaction, while neglecting the larger physical problem such as the gas-particle flowfield. This situation arises owing to the multiple length scales of the problem.

In this work, a numerical solution for dilute gas-particle flows is presented, wherein the effect of the small-scale particle-surface interaction is approximated by statistical particle boundary conditions. This method yields a solution suitable for incompressible flow around or inside any arbitrary two-dimensional body, where particles experience multiple impacts leading to primary and secondary erosion effects.

The numerical method is applied to the cross flow of quartz particles in air over a pipe. This example exhibits the characteristics of aerodynamic bodies with blunt leading edges, as well as the separated regions of recirculating flow common to aerodynamic surfaces with sudden geometrical discontinuities.

Two-Phase Model

The equations which govern the motion of a two-phase mixture are in general quite complex. However, in practice there exist conditions where certain terms of the momentum equations can be neglected. The most significant reduction in complexity occurs when the dispersed phase of particles or droplets is sufficiently dilute in the fluid phase such that the low concentration limits in the governing equations are applicable.

The "principle of correct low concentration limits"[3] states that when the volume fraction of the dispersed phase is much less than unity, the mixture behaves as if it consisted of the fluid phase alone. Thus the equations of motion for the fluid phase reduce to those of an incompressible viscous fluid and take the form of the well-known Navier-Stokes equations. A further implication of the principle of correct low concentration limits is that the forces acting on the dispersed phase must reduce to the expression for the force acting on a single element of the dispersed phase as the volume fraction becomes negligibly small.

In this analysis the mixtures under investigation are dilute since the volume fraction is much less than unity ($0[10^{-3}]$ or less). Two-phase systems such as sand and dust ingestion in jet aircraft and most industrial gas-solid pneumatic transport

Received May 14, 1981.

*Assistant Professor, Department of Mechanical Engineering and Applied Mechanics. Member AIAA.

systems are examples of dilute suspensions. In these situations, the force acting on the particles is dominated by the fluid-induced viscous drag with all other forces such as Basset, Magnus, Brownian, Saffman lift, and virtual mass effects being insignificant.[3]

Furthermore, the relative density of typical solid particles compared to the gas density is large enough so that the pressure force acting on the particle phase is small compared to the drag force upon it.

In nondilute two-phase flow where the relative density is small, the momentum equations are coupled together. For instance, in the motion of sand in water, the sand's inertia affects the water's course and vice versa. But in the case of air-blown sand such as experienced by helicopters in the desert, the air motion is unaffected by the sand's presence.

The governing equations for solid particles suspended dilutely in a gas flow can be written nondimensionally as[3] gas governing equations:

$$\nabla \cdot \boldsymbol{u} = 0 \tag{1a}$$

$$\frac{\partial \boldsymbol{u}}{\partial t} + \boldsymbol{u} \cdot \nabla \boldsymbol{u} = \nabla p + \frac{1}{Re} \nabla^2 \boldsymbol{u} \tag{1b}$$

and particle governing equations:

$$\frac{\partial \alpha_0}{\partial t} + \nabla \cdot (\alpha_0 \boldsymbol{u}_p) = 0 \tag{2a}$$

$$\frac{\partial \boldsymbol{u}_p}{\partial t} + \boldsymbol{u}_p \cdot \nabla \boldsymbol{u}_p = g \frac{(\boldsymbol{u} - \boldsymbol{u}_p)}{\lambda} \tag{2b}$$

where $g = Re_p C_D/24$ is a nondimensional parameter that takes into account the variation of the drag coefficient with particle Reynolds number. By fitting experimental data for the drag coefficients of spherical particles, the following formulas are obtained[4]:

$$C_D = 24(1 + 0.15 Re_p^{0.687})/Re_p \qquad 0 < Re_p \leqq 200$$

$$= 21.94 Re_p^{-0.178} + 0.324 \qquad 200 < Re_p \leqq 2500$$

$$= 0.4 \qquad Re_p > 2500$$

Irregular size particles are sized with the diameter of an equivalent sphere, d, as suggested by Bagnold,[5] where d equals 75% of the mean sieve diameter.

The two other nondimensional parameters in the governing equations are the flow Reynolds number Re and the inertia number λ. Mathematically, a large value of λ results in a solution to the particle's motion that is highly dependent upon the initial conditions.

Physically, this situation indicates that the particles enter and leave a region of interest before there is opportunity for the gas flow to alter the particle's trajectory appreciably. When λ is much less than unity, the particles have sufficient time to adjust to the local gas motion. When λ is on the order of unity, the particles have a memory of events that took place throughout the entire flow domain.

We can write λ in a more tractable form as

$$\lambda = \frac{2}{9} \frac{\rho_p}{\rho} \left(\frac{\sigma}{L}\right)^2 \left(\frac{UL}{\nu}\right)$$

$$= \frac{2}{9} \delta_1 (AR)^2 Re$$

For dilute gas-solids experiments on different scales to be dynamically similar, we require λ/g and Re to be constant between experiments.

Rebound Correlations

Erosion experiments and, more importantly, the actual erosion of turbine blades or other objects, yield a time-space average of the erosion caused by many individual particle impacts. As a particle approaches a surface, it "sees" a rough surface consisting of valleys and hillocks. A particle may strike in a valley and effectively deform the surface, while another particle may strike a hillock of extruded material and remove the hillock's crest. After a period of erosive exposure, a regular ripple pattern of valleys and hillocks may appear which is visible to the unaided eye.[6] The effect of the microscopic geometry has been extensively discussed in the literature.[6-9]

In some cases the initial erosion may improve the performance of turbomachinery and transport systems by polishing the surface material. However, this initial effect is quickly offset by the subsequent material removed, which varies linearly with the quantity of particulates impacting.[2]

In developing a model of the rebound of particles from a surface, similar time-space correlations arise. For instance, a particle directed towards a surface with an apparent impingement angle of nearly 90 deg may impact with an actual impingement angle which is much less, depending on whether the particle impacts in a valley or on a hillock. Also, if the particle rebounds, the rebound angle and velocity are highly dependent on the local initial impingement angle.

To obtain an exact solution of a gas-particle flow over such an irregular microscopic surface is extremely complex; the flow would most likely need a Boltzmann equation description. However this complexity can be circumvented by assuming a functional form for the particle boundary conditions based on experimental evidence.

The laminar gas flow solution is first obtained, assuming a smooth wall due to the negligible effect of surface microgeometry on the gas motion. If the flow is turbulent a solution is obtained using a rough wall. In the numerical solution technique (outlined in the following section) used in this analysis, transition to turbulence is modeled via the stability of vortex elements subject to displacements in an adverse pressure gradient.

Now the apparent effect of an eroded surface on particle trajectories is taken into account by specifying the time-space average experimental rebound conditions.

An experimental study yielding time-space averages was obtained by Grant and Tabakoff[10] by recording many single-particle impacts and rebounds. Owing to the large number of individual particle impacts that need be sampled, only a limited number of cases were evaluated, each with the same materials. These considered the effect of actual angle of impingement on rebound angle and on the coefficient of restitution of velocity. Tests were made on small plates of annealed 2024 aluminum alloy placed in a gas-particle wind tunnel. The impact phenomena of individual quartz particles was recorded at the microsurface using high-speed movies.

A least-squares polynomial curve fit of the mean values of the restitution parameters obtained experimentally[10] for the normal and tangential velocity components is expressed as follows:

$$V_{N_2}/V_{N_1} = 0.993 - 1.76\alpha + 1.56\alpha^2 - 0.49\alpha^3$$

$$V_{T_2}/V_{T_1} = 0.998 - 1.66\alpha + 2.11\alpha^2 - 0.67\alpha^3$$

where α is the actual impingement angle, subscript *1* denotes conditions before impact, and subscript *2* denotes rebound conditions.

The rebound angle which the particle makes with the surface β is given geometrically as

$$\beta = \tan^{-1}\left\{\frac{V_{N_2}}{V_{N_1}} \frac{V_{T_1}}{V_{T_2}} \tan\alpha\right\}$$

These results are highly dependent upon the freestream gas velocity or flow rate, only slightly dependent on particle size,[10] and, as previously discussed, the results are only valid for the particular materials tested. Since the flow rates and particle size tested (200 μ) are within the range where plastic deformation of the test surface occurs, the results are qualitatively applicable to other situations where this mechanism of erosion is evident. However, specific quantitative correlations to different surface materials or particle materials are unwarranted. Furthermore, these results do not indicate the effect of particle fragmentation on impact as reported by Tilly[11] and others.[8] Further work should aim to quantify the dynamic behavior of particle fragmentation.

Although we have statistically masked the exact effect of microscopic geometry, the solution will still yield time and spatial variations in the overall erosion process. One important time-dependent variation occurs owing to the local changes in the gas velocity around a surface. As gas molecules approach the leading edge of a blunt object such as a turbine blade, the gas decelerates to rest at the stagnation point and then accelerates in a direction perpendicular to its original freestream direction. This can result in a local trajectory curvature of small particles such that the erosion at the stagnation point can vary with the gas velocity raised to exponents as high as 4.0.[12]

This high-velocity dependence may even occur for large particles (greater than 20 μ) if the gas flow velocity is low enough so that particle aerodynamic effects (i.e., local trajectory curvature) are prevalent.

These aerodynamic effects can significantly modify the component of a particle's velocity tangential to the surface. This is particularly important because the erosion rate is highly dependent upon the tangential velocity for shallow angle impacts.[10]

Clearly the time and spatial variations due to the gas flow interaction with the surface must be included in an exact analysis. However, since measurements of erosion damage integrate the variation in microscopic surface geometry, we are assured a statistically accurate model of erosion by assuming mean time-space averages of many single-particle impacts.

In this work the rebound correlations are incorporated as a particle boundary condition in a numerical solution of the Navier-Stokes equations. A solution method must take into account boundary-layer growth, separation, and downstream wake effects, since these each play an important role in turbomachinery flows. These viscous effects are initially confined to thin regions near surfaces; thus, it is one intent of this study to determine the interaction of these small regions with the particle rebound phenomena. This viscous flow solution will be applied to the problem of gas-particle cross flow around a pipe (i.e., two-dimensional flow around a cylinder). This problem has been investigated by Glauert,[13] Tilly,[6] and Pettit[14] under the simplifying assumption of inviscid gas flow. Since many investigations have used inviscid potential theory to determine the gas flow, this work will compare the inviscid approximation to the viscous solution given in this work. This work is a first step in determining the accuracy and usefulness of the solution method. Future work will aim at applying the technique to a more complex flow such as a two-stage cascade.

Principle Method of Solution

Several calculation schemes have been developed for a general one-dimensional flow,[15-17] however, much less research has been conducted for two-dimensional flow. The only general two-dimensional model that does not use an inviscid flowfield simplification is the "tank-and-tube" cellular approach developed by Spalding et al.[18] In this method the flowfield is subdivided into a series of "tanks" connected to adjacent tanks by "tubes." Finite-difference equations are derived and solved with the appropriate boundary conditions. This technique has been successfully applied to isothermal flowfields in cyclone separators[19] and electrostatic precipitators.[20]

However, because of the high Reynolds number found in gas turbines, the influence of viscosity is confined to narrow regions close to the surface of bodies. These small regions, which are initially invisible to a finite-difference grid, grow larger particularly if under the influence of an adverse pressure gradient. Qualitatively, the effects of these small regions of boundary-layer backflow are quite pronounced; the flow can become separated from the body by a region of reversed or recirculating flow. Finite-difference schemes produce unreliable results in this situation since the computer cannot store enough grid points falling within the boundary layer to predict boundary-layer growth and subsequent separation satisfactorily. Furthermore, it is often observed that in a boundary layer large truncation errors lead to the formation of an artificial numerical viscosity.[21]

A numerical scheme developed by Chorin,[22] for gas flow only, circumvents these difficulties. The scheme is grid-free in that the vorticity within the fluid is partitioned into vortex "blobs" which are moved according to two components. One component is a random displacement of the vortex blob position; in this way the effect of viscous diffusion is modeled. The other component is a deterministic displacement found by moving the blobs according to their mutual interaction effects. This interaction is determined in a way similar to that in which the motion of point vortices interacting in an inviscid fluid is determined, according to the governing equations of classical hydrodynamics.

Laitone[23] has extended Chorin's vortex technique to a two-phase mixture. Apart from the capacity of the vortex method to simulate the physics of viscous fluids and the process of vorticity injection, the scheme overcomes a major difficulty in modeling the particle phase boundary conditions. Particles striking a surface boundary can either adhere to the surface, leading to particle attrition, or form a bed that slides along the surface, or rebound from the wall. In the vortex method the particles are coagulated into packets[23] which are then followed throughout the flowfield. This Lagrangian description of particles allows precise mathematical consistency with the appropriate physical boundary conditions; in a Eulerian formulation the appropriate conditions at a physical boundary are extremely complicated.[24]

The scheme is applicable to an arbitrary body. The particles are assumed to travel with the gas and with a uniform constant phase density at some initial upstream position. The unsteady equations of motion are solved outside the body with the "no slip" boundary conditions for the gas, and rebound correlations for the particle phase.

The governing equations (1) and (2) are solved by integrating forward in time. At the time step m we assume the gas vorticity distribution and the particle's position and velocity is known. We want to determine the gas vorticity and the particle's position and velocity at the time step $m+1$. Since the flow is incompressible, Poisson's equation is solved using the gas vorticity at the time step $m+1$, yielding the stream function and subsequently the velocity field. This velocity field, which is updated each time, is used to advance the particle's position and velocity.

The vorticity in the gas flowfield is represented by a sum of discrete two-dimensional point vortices with modified finite viscous cores. In this way the induced velocity field of the point vortices remains finite near the origin of the vortex but produces the conventional rotating velocity field that has a speed inversely proportional to the distance from the origin at large distances. The gas momentum equation is solved in two steps. First a solution to Euler's equations is obtained by considering the induced velocity generated at each point vortex by all the others using the Biot-Savart law. This induced velocity is used to displace each vortex through one time step.

Boundaries are created using a panel method which consists of a distribution of sources and sinks. Vorticity is created on the surface of these boundaries and is initialized with a circulation to satisfy the "no slip" condition. This newly created vorticity is allowed to diffuse into the flow domain under the action of a random walk. This is the second step in the solution technique; it yields a solution to the diffusion equation and, when combined with the first step, yields an approximate solution to the Navier-Stokes equations.[22]

Since the gas velocity field is represented entirely by a distribution of modified point vortices, sources, and sinks, a particle's velocity can be determined exactly for any particle position. This is clearly an advantage over a finite-difference solution where the gas velocity is known only at specified grid points, and where the gas velocity must be interpolated for positions away from grid points. In the vortex method the particle's position is integrated forward in time using a fifth-order Runge-Kutta scheme with variable step size to preserve accuracy near boundaries. This technique insures a high degree of resolution in areas of high shear such as separated flow regions. Laitone estimates the maximum error in the particle's velocity as $0(k)+0(Re^{-\frac{1}{2}})$, where k is the time step.[23] Note how the error decreases as the Reynolds number increases, unlike finite-difference schemes.

The particles are initialized at some distance upstream of the object with either a specified slip velocity or the gas freestream velocity. As the particles approach the surface, the step size of the integration is reduced by a factor which can vary up to 100.

Evaluation of the Rebound Phenomena

The rebound correlations previously outlined are here applied to the problem of viscous flow around a cylinder. This geometry is chosen because its behavior is similar to a blunt object near the leading edge. It also exhibits a separated region towards the rear and the accompanying eddy shedding which is common to blades at high angles of attack and objects with rearward-facing sharp corners such as box elbows in piping systems.

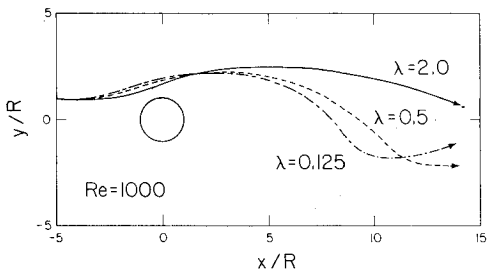

Fig. 1 Particle paths in the near wake region. The Reynolds number is 1000 and the particle inertia number $\lambda=0.125$, 0.5, and 2.0. The time step is 0.2.

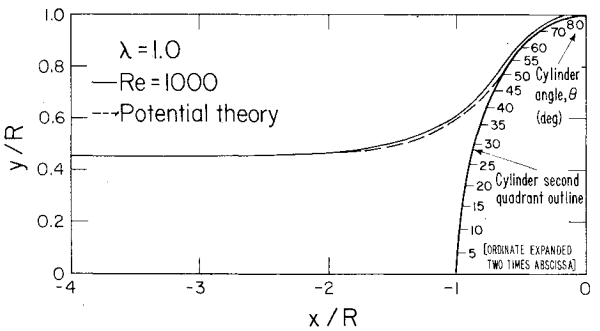

Fig. 2 Particle paths comparing viscous and inviscid flow solutions. In the viscous solution (present method) the particle is deflected over the cylinder. Inviscid solutions overpredict erosion.

The origin is taken at the center of a fixed cylinder with a nondimensional radius of 1. The negative x axis is parallel to the undisturbed stream. The flow is from left to right; at time $t=0$ the flow is started with constant nondimensional velocity of magnitude 1 in the x direction. Thus the velocity at position $(-\infty,0)$ is (1,0). The boundary of the domain, ∂D, is the circumference of the cylinder. The time step is $k=0.2$. The value of k is chosen so that a decrease in k does not affect the flow. The time step must also be small enough so that the particle equations can be integrated without an excessive number of derivative evaluations.

Figure 1 shows the computed trajectories for $Re=1000$ and $\lambda=0.125$, 0.5, and 2.0. The particles, owing to the difference in their inertia, are driven away from the gas streamlines. The higher values of λ, corresponding to bigger or heavier particles, yield particle paths affected less by the gas flow. These larger particles follow more closely straight line trajectories.

By distributing a large number of particles between $y/R=-1.0$ and 1.0, the angle of impact and particle phase density can be calculated as a function of distance along the surface or cylinder angle θ.

Near the stagnation point the vortex method and potential theory yield almost the same impact angles. However, the effect of viscosity becomes apparent for particles impacting at cylinder angles θ greater than 10 deg. The effect of viscosity is to produce a boundary layer and displacement thickness outside of which potential theory adequately describes the flow. But the displacement thickness acts to increase the effective radius of the cylinder. This effect can be seen more clearly in Fig. 2, where a particle with $\lambda=1.0$ is started from the same position ($y/R=0.46$) in a $Re=1000$ and inviscid flow. An inviscid approach used by many investigators[11,13,14] predicts that the particle impacts at $\theta=55$ deg. However, using the present method we find the particle is deflected

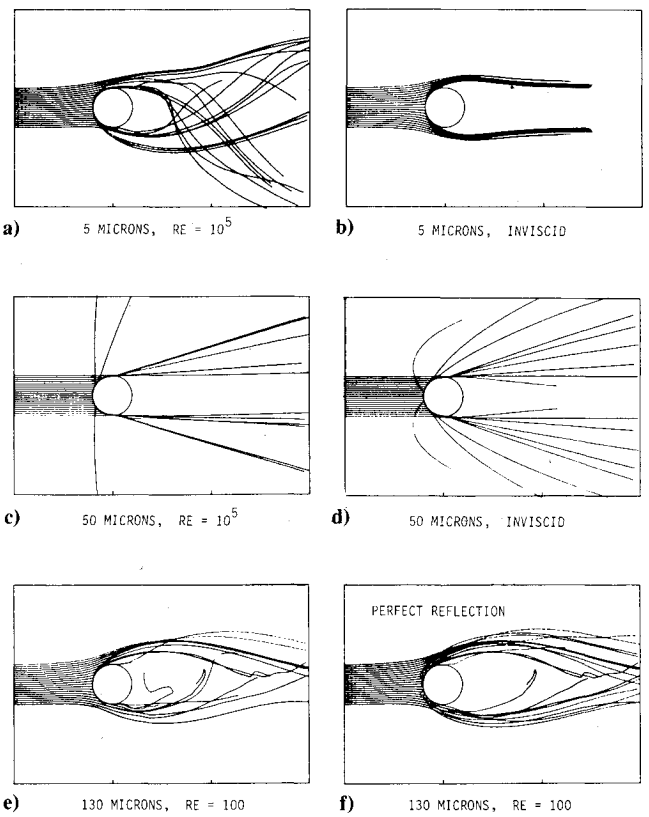

Fig. 3 Particle paths calculated numerically with particle rebound from the cylinder's surface. In the viscous case some particles are captured in the recirculation zone behind the cylinder. The inviscid case is found from potential theory. The viscous Navier-Stokes solution is obtained using a vortex numerical method.

completely around the cylinder with no impact. This is because the present method included viscous boundary-layer effects. In the viscous case the particle path is seen to be displaced away from the cylinder in a uniform way compared to the inviscid case. This simple result suggests an accurate method for utilizing the simplifying assumption of inviscid flow for a particular problem. First, an average displacement thickness, δ^*, should be calculated from boundary-layer theory for the particular geometry and Reynolds number under consideration. Next, the characteristic dimension of the system L should be increased by δ^*. Finally, the inviscid problem should be solved using an equivalent value of the inertia number, namely,

$$\lambda = \frac{2}{9}\frac{\rho_p \sigma^2}{\mu}\left(\frac{U}{L+\delta^*}\right)$$

This will give particle paths corresponding more closely to the viscous case.

We now turn attention towards the back shoulder of the cylinder and the wake region. Shortly after the start of fluid motion, the external pressure field causes fluid transversing the rear shoulder to reverse its direction. This reverse motion moves forward and the boundary layer thickens. This motion gives rise to the vortex which increases in size, until it separates from the cylinder and moves downstream. The vortex method predicts separation occurring asymmetrically and produces the vortex street behind the cylinder. It requires about 20 s of CDC 7600 computer time to follow the particle motion until impact with the cylinder and about 17 min to follow the motion from $t=0$ to 50 in the wake.

In Fig. 3, six plots of particle trajectories and rebound trajectories are shown. Three characteristic rebound phenomena can be seen in Figs. 3a-e: 1) imbedment, 2) single impact and rebound, and 3) multiple impact.

Particle imbedment occurs when a particle strikes the surface and dissipates all of its kinetic energy. Single impacts occur when a particle strikes the surface and dissipates some kinetic energy but still leaves the surface with a modified kinetic energy. In the third case, particles impact the surface two or more times before rebounding free of the surface. These particles tend to bounce across the surface much like a stone skips across the smooth surface of a lake.

These three types of rebound phenomena are qualitatively evident for particles ranging in size from 20 to 500 μ, although the experimental rebound conditions are only quantitatively accurate for a particle size of 200 μ and a Reynolds number of 100,000 (assuming a 2-cm-diam cylinder; this corresponds to a flow velocity of 74.3 m/s).

Figure 3f is identical to Fig. 3e except that a perfect reflection law is assumed as a boundary condition. In this case the angle of impingement equals the angle of rebound and the velocity restitution coefficient is unity. Clearly in Fig. 3f the particles rebound further away from the cylinder and no imbedment occurs. This result demonstrates the significant loss of particle momentum in the erosive case, Fig. 3e. This momentum loss is equivalent to work performed on deforming the surface.

Figures 3a and 3b compare the viscous to inviscid solution. There is a strong focusing of particles behind the cylinder in the viscous case due to eddy shedding. In Fig. 3a, an eddy is shed from the upper shoulder of the cylinder; this eddy has a very strong clockwise rotational motion and creates an upstream force on the particles, deflecting their paths in an upward direction. Computer generated movies of the flow show a regular shedding of eddies accompanied by an upstream movement up or down in the particle paths. The inviscid solution is entirely inadequate in predicting this unsteady result.

Larger particles (greater than 20 μ, as shown in Figs. 3c and 3d) are not affected by the eddy shedding. However, the asymmetry of the viscous solution influences the particle paths in Fig. 3c. The flow Reynolds number is reduced in Figs. 3e and 3f so that, despite the large particle size of 130 μ, the particle's trajectories deflect near the cylinder. The short, twisted paths behind the cylinder identify particles captured in the recirculation zone immediately behind the cylinder. For a 2-cm-diam cylinder the flow velocity in this case is only 7.43 cm/s.

Effect of Particle Velocity

In Fig. 4, a velocity histogram is plotted for a single particle with an inertia number of unity. Recall that this means the particle has a history of past events as well as being significantly influenced by present conditions. This particular example is chosen as illustrative of a typical multiple impact experienced by a particle. The particle impacts and rebounds three times before clearing the top of the cylinder. The nondimensional particle speed is presented historically at each impact point.

At first impact with the cylinder (slightly above the forward stagnation point) the particle's speed is already reduced to about 70% of its freestream value. This is due to gas deflecting around the cylinder; consequently the article "sees" gas at rest relative to its motion, and experiences a retarding force. The impact impingement angle local to the cylinder's surface is 64 deg and the rebound angle is 35 deg.

A surprising result is found at the second impact point, which occurs at 30.3 deg on the cylinder's front shoulder. The impact speed has increased over the rebound speed from the first impact. Evidently the gas flow has had sufficient time to do work on the particle. An acceleration is expected in this case because the gas accelerates away from the stagnation point and reaches a maximum of approximately twice the freestream speed at the top of the cylinder.

This observation is significant in erosion prediction; it means that in flow around blunt objects, particles can obtain a large fraction of their original kinetic energy prior to a secondary impact. Tilly[25] found secondary erosion obtaining significant fractional levels of primary erosion. In Tilly's experiments, particles larger than 30 μ fragmented on impact. This analysis highlights the dependency of secondary erosion on the aerodynamic forces acting throughout a multiple-impact event. The model can be extended to account for fragmentation of particles on impact.

The actual work done on the surface is proportional to the change in momentum of the particle before and after impact. In Fig. 4, the trend is towards a decreasing value of the momentum change after each impact. This implies that the absolute value of erosion is secondary and subsequent impacts will always decrease monotonically; however, the resulting erosion may obtain significant fractional levels of the primary

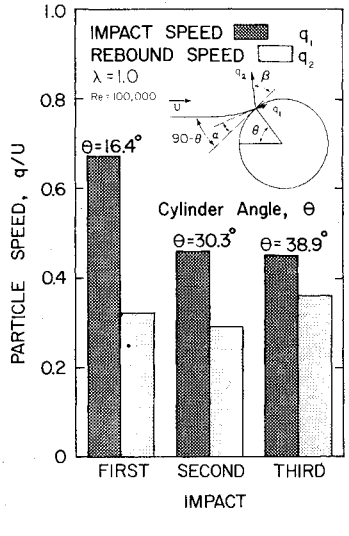

Fig. 4 Particle velocity histogram for a triple impact and rebound with the cylinder's surface. The difference in impact speed and rebound speed is proportional to the momentum lost by the particle in doing erosive work on the surface. Secondary erosion is nearly 50% of primary erosion.

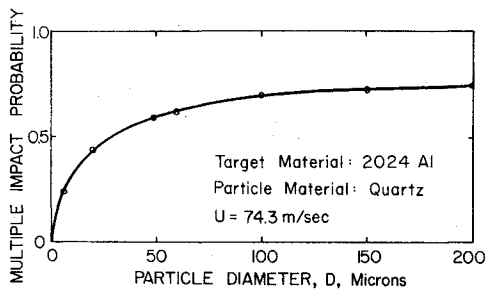

Fig. 5 Numerically predicted probability of multiple impacts occurring for different particle sizes. As the probability of multiple impacts increases, the frequency of secondary erosion increases.

erosion for the aerodynamic reasons described above. Thus in some turbomachinery erosion could perhaps be reduced via changes in aerodynamic design.

Particle Size Effect

Numerical experiments comparing the occurrence of multiple impacts for different particle sizes yielded the data points shown in Fig. 5. Again, it is important to note that this curve is quantitatively accurate only for the specific materials and conditions considered, namely, quartz particles impacting against an aluminum surface. Qualitatively, we expect a similar trend for materials subject to a similar ductile erosion process.

In each test case a fixed number of particles of a uniform size are initially distributed between $y/R = -1$ and 1. This corresponds to a distance of one cylinder diameter. The numerical solution counts the total number of multiple impacts; this is the number of particles which impact the cylinder more than once. This multiple-impact number is divided by the total number of particles present to obtain the fraction of particles that impact more than once. It is more precise to refer to this fraction as the probability of a multiple impact, since the rebound correlations are statistical.

The multiple-impact probability decreases with particle size, with a substantial drop occurring for particles less than 50 μ. The reason for this drop is in part readily explainable: As the particle size decreases, the inertia number decreases; thus the particle trajectory becomes drag dominated. In other words, some particles are carried around the cylinder without impact.

A common example of this is seen on a rainy day. If one drives an automobile out of a rainstorm, it is observed that as the raindrops decrease in size, fewer and fewer will impact on the windshield, since they are deflected over the automobile. Similarly, the smaller erosive particles are deflected around the cylinder. This work does not take into account the well-known size effect in erosion, whereby particles less than 100 μ have substantially reduced erosion efficiency.[2]

The second reason for the decrease in multiple-impact probability depends upon the nature of the rebound correlations. Consider two particles of different sizes initialized in the flow at the same upstream position. The smaller particle will equilibrate with the gas flow faster than the larger particle, so the smaller particle's trajectory will curve slightly resulting in an impact impingement angle on the cylinder always less than that of the larger particle. The experimental rebound correlations [Eq. (5)] predict the rebound velocity restitution coefficient to increase with decreasing impact angle (for impact angles less than 60 deg). Therefore the smaller particle should rebound with a speed close to its impact speed, while the larger particle will rebound at a speed much less than its impact speed.

In the presence of the gas flow, the larger particles will tend to rebound slowly in a direction away from the cylinder, crossing gas streamlines, while the smaller particles rebound quickly with shallow angles following the cylinder's surface and the gas streamlines. This means the small particles travel a longer distance before a second impact, while the larger particles, owing to their low velocity relative to the cylinder, travel a shorter distance until a second impact.

If the particles were assumed to fragment upon impact, and were assumed to roughly obey the rebound correlations used in this study, then the results of Fig. 5 predict that the fragments of large particles have a higher probability of causing secondary erosion. This offers a possible explanation, based on the mechanics of a viscous flow model, for the experimental observation[25] that increasing particle size is associated with an increase in secondary erosion.

Conclusions

It has been the twofold aim of this work to first present a numerical solution technique using statistically simulated particle rebound boundary conditions to obtain an approximate solution for dilute gas-particle flow; and second, to apply the solution technique to a specific geometry and thereby indicate the type of information obtainable that may be useful in erosion analyses.

The descriptive discussion of multiple-impact phenomena, particle size, and velocity effects, suggests possible mechanisms for predicting secondary erosion. The predicted trend demonstrates (within the limited scope of materials and conditions considered) an increase in multiple impacts as particle size increases.

Further work will incorporate different target and particle materials and will apply an erosion model to the numerical solution to enable quantitative erosion predictions.

Work is underway to improve the numerical solution technique in two ways: first, by utilizing a newly devised vortex sheet method[26] that improves the solution near boundaries and, second, by representing the size and velocity variation in the rebound correlations by probability distribution functions. The solution will consist of a Monte Carlo simulation of many individual particles of different sizes.

Future work will include particle-particle collisions and improve mathematical description of the particle phase to include lift forces; this will improve the model's capability to encompass a wider class of two-phase flows.

The computer program used to obtain the results in this work is available from the author.

Acknowledgment

This work was supported by the Division of Materials Science, Office of Basic Research, U.S. Department of Energy, under Contract W-7405-ENG-48.

References

[1] Taylor, G.I., "Notes of Possible Equipment and Technique for Experiments Experiments on Icing of Aircraft," Aeronautical Research Committee, R&M, No. 2024, 1940, pp. 1-7.

[2] Tilly, G.P., "The Significance of Particle Size in Sand Erosion of Small Gas Turbines," *The Aeronautical Journal of the Royal Aeronautical Society,* Vol. 73, 1969, pp. 427-428.

[3] Drew, D.A., "Two-Phase Flows: Constitutive Equations for Lift and Brownian Motion and Some Basic Flows," *Archive for Rational Mechanics,* Vol. 62, No. 2, 1976, pp. 149-163.

[4] Boothroyd, R. G., *Flowing Gas-Solids Suspensions,* Chapman and Hall, London, 1971.

[5] Bagnold, R.A., *The Physics of Wind Blown Sands and Desert Dunes,* Methuen, London, 1960.

[6] Tilly, G. P., "Erosion Caused by Airborne Particles," *Wear,* Vol. 14, 1969, pp. 63-79.

[7] Finnie, I., "Some Observations on the Erosion of Ductile Metals," *Wear,* Vol. 19, 1972, pp. 81-90.

[8] Ruff, A.W. and Wiederhorn, S.M., "Erosion by Solid Particle Impact," *Treatise on Material Science and Technology,* Vol. 16, 1980, pp. 69-126.

[9] Hussein, M.F., "The Dynamic Characteristics of Solid Particles in Particulate Flow in Rotating Turbomachinery," Ph.D. Dissertation, University of Cincinnati, Cincinnati, Ohio, 1972.

[10]Grant, G. and Tabakoff, W., "Erosion Prediction in Turbomachinery Resulting from Environmental Solid Particles," *Journal of Aircraft,* Vol. 12, May 1975, pp. 471-478.

[11]Tilly, G.P. and Sage, W., "The Interaction of Particle and Material Behaviour in Erosion Processes," *Wear,* Vol. 16, 1970, pp. 447-465.

[12]Laitone, J.A., "Erosion Prediction Near a Stagnation Point Resulting from Aerodynamically Entrained Solid Particles," *Journal of Aircraft,* Vol. 16, Dec. 1979, pp. 809-814.

[13]Glauert, M., "A method of constructing the paths of raindrops of different diameters moving in the neighborhood of (1) a circular cylinder, (2) an airfoil, placed in a uniform stream of air; and a determination of the rate of deposit of the drops on the surface and the percentage of drops caught," Aeronautical Research Committee, R&M, No. 2025, 1940.

[14]Pettit, F.S. and Barkalow, R.H., "Design of Materials for Use Under Erosion/Corrosion Conditions at High Temperatures in Coal Gasification and Coal Combustion Systems," Pratt and Whitney Aircraft, East Hartford, Conn., 75-200-7107-6, May 1977.

[15]Crowe, C.T. et al., "Dynamics of Two-Phase Flow in Rocket Nozzles," United Technologies Report 2102-FR, Sept. 1965.

[16]Kliegel, J.S., "One-Dimensional Flow of Gas-Particle System," IAS Paper 60-65, 1960.

[17]Wallis, G.B., *One-Dimensional Two-Phase Flow,* McGraw-Hill, New York, 1969.

[18]Gosman, A.D. et al., *Heat and Mass Transfer in Recirculating Flows,* Academic Press, New York, 1969.

[19]Crowe, C.T. and Pratt, D.T., "Analysis of the Flow Field in Cyclone Separators," Paper 2B(4) presented at the Symposium on Application of Computers to Fluid Dynamic Analysis and Design, Polytechnic Institute of Brooklyn, Brooklyn, N.Y., 1973.

[20]Stock, D.E. and Crowe, C.T., "Analysis of the Flow Field in Electrostatic Precipitators," Paper presented at the Spring Meeting of the Mid Western Section of the Combustion Institute, 1973.

[21]Dorodnicyn, A.A., "Review of Methods for Solving Navier-Stokes Equations," *Proceedings of IIIrd International Conference on Numerical Methods in Fluid Mechanics, Lecture Notes in Physics,* Springer-Verlag, Berlin, 1973, pp. 1-11.

[22]Chorin, A.J., "Numerical Study of Slightly Viscous Flow," *Journal of Fluid Mechanics,* Vol. 57, 1973, pp. 785-796.

[23]Laitone, J.A., "Numerical Solution of Gas-Particle Flows at High Reynolds Numbers," to be published in *Journal of Applied Mechanics.*

[24]Yeung, W.S., "Fundamentals of the Particulate Phase in a Gas-Solid Mixture," Lawrence Berkeley Laboratory, Berkeley, Calif., Report No. LBL-8440, 1978.

[25]Tilly, G.P., "A Two Stage Mechanism of Ductile Erosion," *Wear,* Vol. 23, 1973, pp. 87-96.

[26]Chorin, A.J., "Vortex Sheet Approximation of Boundary Layers," *Journal of Computational Physics,* Vol. 27, No. 3, 1978, pp. 428-442.